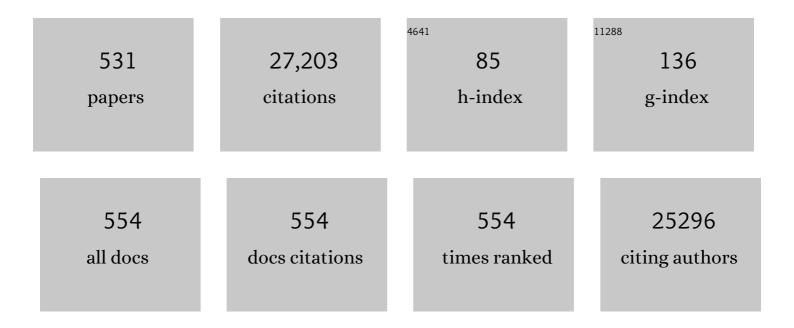
List of Publications by Year in descending order

Source: https://exaly.com/author-pdf/886093/publications.pdf Version: 2024-02-01



#	Article	IF	CITATIONS
1	Carrier dynamics in semiconductors studied with time-resolved terahertz spectroscopy. Reviews of Modern Physics, 2011, 83, 543-586.	16.4	978
2	Cooperativity in Ion Hydration. Science, 2010, 328, 1006-1009.	6.0	562
3	Photoexcitation cascade and multiple hot-carrier generation in graphene. Nature Physics, 2013, 9, 248-252.	6.5	512
4	Synthesis of structurally well-defined and liquid-phase-processable graphene nanoribbons. Nature Chemistry, 2014, 6, 126-132.	6.6	468
5	Phonon- Versus Electron-Mediated Desorption and Oxidation of CO on Ru(0001). Science, 1999, 285, 1042-1045.	6.0	443
6	Boosting Power Conversion Efficiencies of Quantum-Dot-Sensitized Solar Cells Beyond 8% by Recombination Control. Journal of the American Chemical Society, 2015, 137, 5602-5609.	6.6	367
7	Extremely efficient terahertz high-harmonic generation in graphene by hot Dirac fermions. Nature, 2018, 561, 507-511.	13.7	365
8	Local Field Effects on Electron Transport in Nanostructured TiO2 Revealed by Terahertz Spectroscopy. Nano Letters, 2006, 6, 755-759.	4.5	351
9	High-mobility band-like charge transport in a semiconducting two-dimensional metal–organic framework. Nature Materials, 2018, 17, 1027-1032.	13.3	341
10	Vibrational Spectroscopy and Dynamics of Water. Chemical Reviews, 2016, 116, 7590-7607.	23.0	300
11	Vibrational Response of Hydrogen-Bonded Interfacial Water is Dominated by Intramolecular Coupling. Physical Review Letters, 2008, 100, 173901.	2.9	296
12	Assessment of carrier-multiplication efficiency in bulk PbSe and PbS. Nature Physics, 2009, 5, 811-814.	6.5	245
13	Unified Molecular View of the Air/Water Interface Based on Experimental and Theoretical χ ⁽²⁾ Spectra of an Isotopically Diluted Water Surface. Journal of the American Chemical Society, 2011, 133, 16875-16880.	6.6	245
14	Unveiling Electronic Properties in Metal–Phthalocyanine-Based Pyrazine-Linked Conjugated Two-Dimensional Covalent Organic Frameworks. Journal of the American Chemical Society, 2019, 141, 16810-16816.	6.6	227
15	Sulfurâ€Enriched Conjugated Polymer Nanosheet Derived Sulfur and Nitrogen coâ€Doped Porous Carbon Nanosheets as Electrocatalysts for Oxygen Reduction Reaction and Zinc–Air Battery. Advanced Functional Materials, 2016, 26, 5893-5902.	7.8	214
16	Direct extraction of Raman line-shapes from congested CARS spectra. Optics Express, 2006, 14, 3622.	1.7	210
17	Quantitative Label-Free Imaging of Lipid Composition and Packing of Individual Cellular Lipid Droplets Using Multiplex CARS Microscopy. Biophysical Journal, 2008, 95, 4908-4914.	0.2	205
18	Electron transport inTiO2probed by THz time-domain spectroscopy. Physical Review B, 2004, 69, .	1.1	203

#	Article	IF	CITATIONS
19	Direct Observation of Electron-to-Hole Energy Transfer in CdSe Quantum Dots. Physical Review Letters, 2006, 96, 057408.	2.9	197
20	Ultrafast electron dynamics at metal surfaces: Competition between electron-phonon coupling and hot-electron transport. Physical Review B, 2000, 61, 1101-1105.	1.1	187
21	Liquid flow along a solid surface reversibly alters interfacial chemistry. Science, 2014, 344, 1138-1142.	6.0	187
22	Phonon–Electron Scattering Limits Free Charge Mobility in Methylammonium Lead Iodide Perovskites. Journal of Physical Chemistry Letters, 2015, 6, 4991-4996.	2.1	186
23	Water at charged interfaces. Nature Reviews Chemistry, 2021, 5, 466-485.	13.8	186
24	Efficiency of Exciton and Charge Carrier Photogeneration in a Semiconducting Polymer. Physical Review Letters, 2004, 92, 196601.	2.9	183
25	lce-nucleating bacteria control the order and dynamics of interfacial water. Science Advances, 2016, 2, e1501630.	4.7	182
26	Ultrafast vibrational energy transfer at the water/air interface revealed by two-dimensional surface vibrational spectroscopy. Nature Chemistry, 2011, 3, 888-893.	6.6	177
27	Femtosecond Surface Vibrational Spectroscopy of CO Adsorbed on Ru(001) during Desorption. Physical Review Letters, 2000, 84, 4653-4656.	2.9	175
28	The Bending Mode of Water: A Powerful Probe for Hydrogen Bond Structure of Aqueous Systems. Journal of Physical Chemistry Letters, 2020, 11, 8459-8469.	2.1	175
29	Carrier Multiplication and Its Reduction by Photodoping in Colloidal InAs Quantum Dots. Journal of Physical Chemistry C, 2007, 111, 4146-4152.	1.5	172
30	Real-Time Observation of Molecular Motion on a Surface. Science, 2005, 310, 1790-1793.	6.0	167
31	Dielectric Relaxation Dynamics of Water in Model Membranes Probed by Terahertz Spectroscopy. Biophysical Journal, 2009, 97, 2484-2492.	0.2	166
32	Single-shot measurement of terahertz electromagnetic pulses by use of electro-optic sampling. Optics Letters, 2000, 25, 426.	1.7	163
33	Vibrational Spectroscopic Investigation of the Phase Diagram of a Biomimetic Lipid Monolayer. Physical Review Letters, 2003, 90, 128101.	2.9	159
34	On the Absence of Detectable Carrier Multiplication in a Transient Absorption Study of InAs/CdSe/ZnSe Core/Shell1/Shell2 Quantum Dots. Nano Letters, 2008, 8, 1207-1211.	4.5	159
35	Nonlinear optical scattering: The concept of effective susceptibility. Physical Review B, 2004, 70, .	1.1	150
36	Ultrafast surface vibrational dynamics. Surface Science Reports, 2010, 65, 45-66.	3.8	148

#	Article	IF	CITATIONS
37	Thermodynamic picture of ultrafast charge transport in graphene. Nature Communications, 2015, 6, 7655.	5.8	147
38	Exciton polarizability in semiconductor nanocrystals. Nature Materials, 2006, 5, 861-864.	13.3	146
39	Coordination Polymer Framework Based Onâ€Chip Microâ€Supercapacitors with AC Lineâ€Filtering Performance. Angewandte Chemie - International Edition, 2017, 56, 3920-3924.	7.2	140
40	Bottom-Up Synthesis of Liquid-Phase-Processable Graphene Nanoribbons with Near-Infrared Absorption. ACS Nano, 2014, 8, 11622-11630.	7.3	138
41	Hydrogen bonding strength of interfacial water determined with surface sum-frequency generation. Chemical Physics Letters, 2009, 470, 7-12.	1.2	137
42	Vibrational Sum Frequency Scattering from a Submicron Suspension. Physical Review Letters, 2003, 91, 258302.	2.9	135
43	Molecular Structure and Dynamics of Water at the Water–Air Interface Studied with Surfaceâ€Specific Vibrational Spectroscopy. Angewandte Chemie - International Edition, 2015, 54, 5560-5576.	7.2	132
44	Strong frequency dependence of vibrational relaxation in bulk and surface water reveals sub-picosecond structural heterogeneity. Nature Communications, 2015, 6, 8384.	5.8	132
45	Experimental and theoretical evidence for bilayer-by-bilayer surface melting of crystalline ice. Proceedings of the National Academy of Sciences of the United States of America, 2017, 114, 227-232.	3.3	131
46	Out-of-plane heat transfer in van der Waals stacks through electron–hyperbolic phonon coupling. Nature Nanotechnology, 2018, 13, 41-46.	15.6	128
47	Complex Formation in Aqueous Trimethylamine- <i>N</i> -oxide (TMAO) Solutions. Journal of Physical Chemistry B, 2012, 116, 4783-4795.	1.2	127
48	Optical Control over Surface-Plasmon-Polariton-Assisted THz Transmission through a Slit Aperture. Physical Review Letters, 2008, 100, 123901.	2.9	125
49	Influence of Concentration and Temperature on the Dynamics of Water in the Hydrophobic Hydration Shell of Tetramethylurea. Journal of the American Chemical Society, 2010, 132, 15671-15678.	6.6	124
50	Quantifying Polaron Formation and Charge Carrier Cooling in Leadâ€lodide Perovskites. Advanced Materials, 2018, 30, e1707312.	11.1	124
51	Ultra-broadband THz time-domain spectroscopy of common polymers using THz air photonics. Optics Express, 2014, 22, 12475.	1.7	121
52	Quantitative Coherent Anti-Stokes Raman Scattering (CARS) Microscopy. Journal of Physical Chemistry B, 2011, 115, 7713-7725.	1.2	120
53	A semiconducting layered metal-organic framework magnet. Nature Communications, 2019, 10, 3260.	5.8	119
54	The Polyphenol EGCG Inhibits Amyloid Formation Less Efficiently at Phospholipid Interfaces than in Bulk Solution. Journal of the American Chemical Society, 2012, 134, 14781-14788.	6.6	118

#	Article	IF	CITATIONS
55	Ultrafast Photoconductivity of Graphene Nanoribbons and Carbon Nanotubes. Nano Letters, 2013, 13, 5925-5930.	4.5	117
56	Structure and Dynamics of Interfacial Peptides and Proteins from Vibrational Sum-Frequency Generation Spectroscopy. Chemical Reviews, 2020, 120, 3420-3465.	23.0	114
57	High-Mobility Semiconducting Two-Dimensional Conjugated Covalent Organic Frameworks with <i>p</i> -Type Doping. Journal of the American Chemical Society, 2020, 142, 21622-21627.	6.6	113
58	Morphology and Persistence Length of Amyloid Fibrils Are Correlated to Peptide Molecular Structure. Journal of the American Chemical Society, 2011, 133, 18030-18033.	6.6	112
59	Interchain effects in the ultrafast photophysics of a semiconducting polymer:THztime-domain spectroscopy of thin films and isolated chains in solution. Physical Review B, 2005, 71, .	1.1	110
60	Calcium-Induced Phospholipid Ordering Depends on Surface Pressure. Journal of the American Chemical Society, 2007, 129, 11079-11084.	6.6	110
61	Molecular hydrophobicity at a macroscopically hydrophilic surface. Proceedings of the National Academy of Sciences of the United States of America, 2019, 116, 1520-1525.	3.3	109
62	Anisotropic Water Reorientation around Ions. Journal of Physical Chemistry B, 2011, 115, 12638-12647.	1.2	108
63	Aqueous Heterogeneity at the Air/Water Interface Revealed by 2Dâ€HD‧FG Spectroscopy. Angewandte Chemie - International Edition, 2014, 53, 8146-8149.	7.2	106
64	Accessing the fundamentals of magnetotransport in metals with terahertz probes. Nature Physics, 2015, 11, 761-766.	6.5	103
65	Desorption of CO from Ru(001) induced by near-infrared femtosecond laser pulses. Journal of Chemical Physics, 2000, 112, 9888-9897.	1.2	102
66	Ultrafast Vibrational Energy Transfer between Surface and Bulk Water at the Air-Water Interface. Physical Review Letters, 2007, 98, 098302.	2.9	102
67	Water orientation and hydrogen-bond structure at the fluorite/water interface. Scientific Reports, 2016, 6, 24287.	1.6	101
68	Both Inter- and Intramolecular Coupling of O–H Groups Determine the Vibrational Response of the Water/Air Interface. Journal of Physical Chemistry Letters, 2016, 7, 4591-4595.	2.1	101
69	Water Bending Mode at the Water–Vapor Interface Probed by Sum-Frequency Generation Spectroscopy: A Combined Molecular Dynamics Simulation and Experimental Study. Journal of Physical Chemistry Letters, 2013, 4, 1872-1877.	2.1	100
70	Toward <i>ab initio</i> molecular dynamics modeling for sum-frequency generation spectra; an efficient algorithm based on surface-specific velocity-velocity correlation function. Journal of Chemical Physics, 2015, 143, 124702.	1.2	100
71	Highly Crystalline and Semiconducting Imineâ€Based Twoâ€Dimensional Polymers Enabled by Interfacial Synthesis. Angewandte Chemie - International Edition, 2020, 59, 6028-6036.	7.2	98
72	Quantitative CARS Molecular Fingerprinting of Single Living Cells with the Use of the Maximum Entropy Method. Angewandte Chemie - International Edition, 2010, 49, 6773-6777.	7.2	97

#	Article	IF	CITATIONS
73	Competing Ultrafast Energy Relaxation Pathways in Photoexcited Graphene. Nano Letters, 2014, 14, 5839-5845.	4.5	97
74	Extreme surface propensity of halide ions in water. Nature Communications, 2014, 5, 4083.	5.8	97
75	IM30 triggers membrane fusion in cyanobacteria and chloroplasts. Nature Communications, 2015, 6, 7018.	5.8	97
76	Terahertz Nonlinear Optics of Graphene: From Saturable Absorption to Highâ€Harmonics Generation. Advanced Optical Materials, 2020, 8, 1900771.	3.6	97
77	Molecular Structure and Modeling of Water–Air and Ice–Air Interfaces Monitored by Sum-Frequency Generation. Chemical Reviews, 2020, 120, 3633-3667.	23.0	97
78	Photoswitchable Micro-Supercapacitor Based on a Diarylethene-Graphene Composite Film. Journal of the American Chemical Society, 2017, 139, 9443-9446.	6.6	96
79	A Molecular View of Cholesterol-Induced Condensation in a Lipid Monolayer. Journal of Physical Chemistry B, 2004, 108, 19083-19085.	1.2	95
80	THz dielectric relaxation of ionic liquid:water mixtures. Chemical Physics Letters, 2007, 439, 60-64.	1.2	95
81	Ultrafast Two Dimensional-Infrared Spectroscopy of a Molecular Monolayer. Journal of the American Chemical Society, 2008, 130, 2152-2153.	6.6	95
82	The ultrafast dynamics and conductivity of photoexcited graphene at different Fermi energies. Science Advances, 2018, 4, eaar5313.	4.7	95
83	Structure Dynamics of the Proton in Liquid Water Probed with Terahertz Time-Domain Spectroscopy. Physical Review Letters, 2009, 102, 198303.	2.9	91
84	Surface-specific vibrational spectroscopy of the water/silica interface: screening and interference. Physical Chemistry Chemical Physics, 2017, 19, 16875-16880.	1.3	91
85	Role of Dielectric Drag in Polaron Mobility in Lead Halide Perovskites. ACS Energy Letters, 2017, 2, 2555-2562.	8.8	90
86	Interface-Specific Ultrafast Two-Dimensional Vibrational Spectroscopy. Accounts of Chemical Research, 2009, 42, 1332-1342.	7.6	89
87	Amyloids: From molecular structure to mechanical properties. Polymer, 2013, 54, 2473-2488.	1.8	89
88	Chemisorbed and Physisorbed Water at the TiO ₂ /Water Interface. Journal of Physical Chemistry Letters, 2017, 8, 2195-2199.	2.1	89
89	Charge Transport and Carrier Dynamics in Liquids Probed by THz Time-Domain Spectroscopy. Physical Review Letters, 2001, 86, 340-343.	2.9	88
90	Chemical Vapor Deposition Synthesis and Terahertz Photoconductivity of Low-Band-Gap <i>N</i> = 9 Armchair Graphene Nanoribbons. Journal of the American Chemical Society, 2017, 139, 3635-3638.	6.6	88

#	Article	IF	CITATIONS
91	On the origin of the extremely different solubilities of polyethers in water. Nature Communications, 2019, 10, 2893.	5.8	88
92	Quantitative CARS Spectroscopy Using the Maximum Entropy Method: The Main Lipid Phase Transition. ChemPhysChem, 2007, 8, 279-287.	1.0	86
93	Coulomb explosion in femtosecond laser ablation of Si(111). Applied Physics Letters, 2003, 82, 4190-4192.	1.5	84
94	Ultrafast Reorientation of Dangling OH Groups at the Air-Water Interface Using Femtosecond Vibrational Spectroscopy. Physical Review Letters, 2011, 107, 116102.	2.9	84
95	Membrane-Bound Water is Energetically Decoupled from Nearby Bulk Water:  An Ultrafast Surface-Specific Investigation. Journal of the American Chemical Society, 2007, 129, 9608-9609.	6.6	83
96	Tuning Electron Transfer Rates through Molecular Bridges in Quantum Dot Sensitized Oxides. Nano Letters, 2013, 13, 5311-5315.	4.5	83
97	Determining Absolute Molecular Orientation at Interfaces: A Phase Retrieval Approach for Sum Frequency Generation Spectroscopy. Journal of Physical Chemistry C, 2009, 113, 6100-6106.	1.5	82
98	Structural Inhomogeneity of Interfacial Water at Lipid Monolayers Revealed by Surface-Specific Vibrational Pumpâ "Probe Spectroscopy. Journal of the American Chemical Society, 2010, 132, 14971-14978.	6.6	82
99	Surface Crystallization of Amorphous Solid Water. Physical Review Letters, 2004, 92, 236101.	2.9	81
100	Determining In Situ Protein Conformation and Orientation from the Amide-I Sum-Frequency Generation Spectrum: Theory and Experiment. Journal of Physical Chemistry A, 2013, 117, 6311-6322.	1.1	81
101	Dynamic Surface Tension of Surfactants in the Presence of High Salt Concentrations. Langmuir, 2020, 36, 7956-7964.	1.6	81
102	Ultrafast optical switching of the THz transmission through metallic subwavelength hole arrays. Physical Review B, 2007, 75, .	1.1	80
103	Carrier multiplication in bulk and nanocrystalline semiconductors: Mechanism, efficiency, and interest for solar cells. Physical Review B, 2010, 81, .	1.1	80
104	Nuclear Quantum Effects Affect Bond Orientation of Water at the Water-Vapor Interface. Physical Review Letters, 2012, 109, 226101.	2.9	79
105	Genetically encoded lipid–polypeptide hybrid biomaterials that exhibit temperature-triggered hierarchical self-assembly. Nature Chemistry, 2018, 10, 496-505.	6.6	79
106	Exciton and electron-hole plasma formation dynamics in ZnO. Physical Review B, 2007, 76, .	1.1	77
107	Mechanism of vibrational energy dissipation of free OH groups at the air–water interface. Proceedings of the National Academy of Sciences of the United States of America, 2013, 110, 18780-18785.	3.3	77
108	Saturation of charge-induced water alignment at model membrane surfaces. Science Advances, 2018, 4, eaap7415.	4.7	76

#	Article	IF	CITATIONS
109	Observation of buried water molecules in phospholipid membranes by surface sum-frequency generation spectroscopy. Journal of Chemical Physics, 2009, 131, 161107.	1.2	75
110	The Role of Intact Oleosin for Stabilization and Function of Oleosomes. Journal of Physical Chemistry B, 2013, 117, 13872-13883.	1.2	75
111	Molecular Mechanism of Water Evaporation. Physical Review Letters, 2015, 115, 236102.	2.9	75
112	Label-Free Imaging of Lipophilic Bioactive Molecules during Lipid Digestion by Multiplex Coherent Anti-Stokes Raman Scattering Microspectroscopy. Journal of the American Chemical Society, 2010, 132, 8433-8439.	6.6	74
113	Single-pulse terahertz coherent control of spin resonance in the canted antiferromagnet YFeO <mml:math <br="" xmlns:mml="http://www.w3.org/1998/Math/MathML">display="inline"><mml:msub><mml:mrow></mml:mrow><mml:mn>3</mml:mn></mml:msub></mml:math> , mediated by dielectric anisotropy. Physical Review B. 2013. 87	1.1	74
114	Lipid Carbonyl Groups Terminate the Hydrogen Bond Network of Membrane-Bound Water. Journal of Physical Chemistry Letters, 2015, 6, 4499-4503.	2.1	74
115	Comparative Study of Direct and Phase-Specific Vibrational Sum-Frequency Generation Spectroscopy: Advantages and Limitations. Journal of Physical Chemistry B, 2011, 115, 15362-15369.	1.2	73
116	Label-free characterization of biomembranes: from structure to dynamics. Chemical Society Reviews, 2014, 43, 887-900.	18.7	72
117	Tuning the Structural and Optoelectronic Properties of Cs ₂ AgBiBr ₆ Doubleâ€Perovskite Single Crystals through Alkaliâ€Metal Substitution. Advanced Materials, 2020, 32, e2001878.	11.1	72
118	Ultrafast active control of localized surface plasmon resonances in silicon bowtie antennas. Optics Express, 2010, 18, 23226.	1.7	70
119	Water-mediated interactions between trimethylamine-N-oxide and urea. Physical Chemistry Chemical Physics, 2015, 17, 298-306.	1.3	70
120	Nanoscale Heterogeneity of the Molecular Structure of Individual hIAPP Amyloid Fibrils Revealed with Tipâ€Enhanced Raman Spectroscopy. Small, 2015, 11, 4131-4139.	5.2	69
121	Grating-Graphene Metamaterial as a Platform for Terahertz Nonlinear Photonics. ACS Nano, 2021, 15, 1145-1154.	7.3	69
122	Sensitive Probing of DNA Binding to a Cationic Lipid Monolayer. Journal of the American Chemical Society, 2007, 129, 8420-8421.	6.6	68
123	Coupling between intra- and intermolecular motions in liquid water revealed by two-dimensional terahertz-infrared-visible spectroscopy. Nature Communications, 2018, 9, 885.	5.8	67
124	Measurement of the Frequency-Dependent Conductivity in Sapphire. Physical Review Letters, 2003, 90, 247401.	2.9	66
125	Labelâ€Free Chemical Imaging of Catalytic Solids by Coherent Antiâ€&tokes Raman Scattering and Synchrotronâ€Based Infrared Microscopy. Angewandte Chemie - International Edition, 2009, 48, 8990-8994.	7.2	65
126	Hydrogen-Bond Dynamics in a Protic Ionic Liquid: Evidence of Large-Angle Jumps. Journal of Physical Chemistry Letters, 2012, 3, 3034-3038.	2.1	65

#	Article	IF	CITATIONS
127	On the Role of Fresnel Factors in Sum-Frequency Generation Spectroscopy of Metal–Water and Metal-Oxide–Water Interfaces. Journal of Physical Chemistry C, 2012, 116, 23351-23361.	1.5	65
128	Lateral Fusion of Chemical Vapor Deposited <i>N</i> = 5 Armchair Graphene Nanoribbons. Journal of the American Chemical Society, 2017, 139, 9483-9486.	6.6	65
129	Time- vs. frequency-domain femtosecond surface sum frequency generation. Chemical Physics Letters, 2003, 370, 227-232.	1.2	64
130	Quantitative Multiplex CARS Spectroscopy in Congested Spectral Regions. Journal of Physical Chemistry B, 2006, 110, 4472-4479.	1.2	64
131	Role of Edge Engineering in Photoconductivity of Graphene Nanoribbons. Journal of the American Chemical Society, 2017, 139, 7982-7988.	6.6	64
132	Picosecond Electron Injection Dynamics in Dye-Sensitized Oxides in the Presence of Electrolyte. Journal of Physical Chemistry C, 2011, 115, 2578-2584.	1.5	63
133	Direct observation of mode-specific phonon-band gap coupling in methylammonium lead halide perovskites. Nature Communications, 2017, 8, 687.	5.8	63
134	Molecular Insight into the Slipperiness of Ice. Journal of Physical Chemistry Letters, 2018, 9, 2838-2842.	2.1	63
135	Anomalous Independence of Multiple Exciton Generation on Different Group IVâ^'VI Quantum Dot Architectures. Nano Letters, 2011, 11, 1623-1629.	4.5	61
136	Ultrafast terahertz magnetometry. Nature Communications, 2020, 11, 4247.	5.8	61
137	Laser-Heating-Induced Displacement of Surfactants on the Water Surface. Journal of Physical Chemistry B, 2012, 116, 2703-2712.	1.2	60
138	Serotonergic innervation and serotonin receptor expression of NPY-producing neurons in the rat lateral and basolateral amygdaloid nuclei. Brain Structure and Function, 2013, 218, 421-435.	1.2	60
139	The surface roughness, but not the water molecular orientation varies with temperature at the water–air interface. Physical Chemistry Chemical Physics, 2015, 17, 23559-23564.	1.3	60
140	Interfacial Approach toward Benzeneâ€Bridged Polypyrrole Film–Based Microâ€Supercapacitors with Ultrahigh Volumetric Power Density. Advanced Functional Materials, 2020, 30, 1908243.	7.8	60
141	Long-lived charge separation following pump-wavelength–dependent ultrafast charge transfer in graphene/WS ₂ heterostructures. Science Advances, 2021, 7, .	4.7	60
142	Direct Observation of Vibrational Energy Delocalization on Surfaces: CO on Ru(001). Physical Review Letters, 2000, 85, 4341-4344.	2.9	59
143	The Interaction of Water with the Pt(533) Surface. Journal of Physical Chemistry B, 2004, 108, 12575-12582.	1.2	59
144	Two Types of Water at the Water–Surfactant Interface Revealed by Time-Resolved Vibrational Spectroscopy Journal of the American Chemical Society, 2015, 137, 14912-14919	6.6	58

#	Article	IF	CITATIONS
145	Surface molecular view of colloidal gelation. Proceedings of the National Academy of Sciences of the United States of America, 2006, 103, 13310-13314.	3.3	57
146	Picosecond orientational dynamics of water in living cells. Nature Communications, 2017, 8, 904.	5.8	57
147	The Surface of Ice under Equilibrium and Nonequilibrium Conditions. Accounts of Chemical Research, 2019, 52, 1006-1015.	7.6	57
148	Kinetic Control over Self-Assembly of Semiconductor Nanoplatelets. Nano Letters, 2020, 20, 4102-4110.	4.5	57
149	Probing the charge separation process on In 2 S 3 /Pt-TiO 2 nanocomposites for boosted visible-light photocatalytic hydrogen production. Applied Catalysis B: Environmental, 2016, 198, 25-31.	10.8	56
150	Probing the Mineral–Water Interface with Nonlinear Optical Spectroscopy. Angewandte Chemie - International Edition, 2021, 60, 10482-10501.	7.2	56
151	The dynamics of vibrational excitations on surfaces: CO on Ru(001). Journal of Chemical Physics, 2001, 115, 7725-7735.	1.2	55
152	Reduction of carrier mobility in semiconductors caused by charge-charge interactions. Physical Review B, 2007, 75, .	1.1	55
153	Simulation studies of pore and domain formation in a phospholipid monolayer. Journal of Chemical Physics, 2005, 122, 024704.	1.2	54
154	Small Size, Big Impact: Recent Progress in Bottomâ€Up Synthesized Nanographenes for Optoelectronic and Energy Applications. Advanced Science, 2022, 9, e2106055.	5.6	54
155	Novel Surface Vibrational Spectroscopy: Infrared-Infrared-Visible Sum-Frequency Generation. Physical Review Letters, 2001, 86, 1566-1569.	2.9	53
156	Size-Dependent Electron Transfer from PbSe Quantum Dots to SnO2Monitored by Picosecond Terahertz Spectroscopy. Nano Letters, 2011, 11, 5234-5239.	4.5	53
157	Observation and Identification of a New OH Stretch Vibrational Band at the Surface of Ice. Journal of Physical Chemistry Letters, 2017, 8, 3656-3660.	2.1	53
158	Conductivity of solvated electrons in hexane investigated with terahertz time-domain spectroscopy. Journal of Chemical Physics, 2004, 121, 394.	1.2	52
159	Ultrafast Terahertz Photoconductivity of Photovoltaic Polymer–Fullerene Blends: A Comparative Study Correlated with Photovoltaic Device Performance. Journal of Physical Chemistry Letters, 2014, 5, 3662-3668.	2.1	52
160	Reversible Activation of a Cell-Penetrating Peptide in a Membrane Environment. Journal of the American Chemical Society, 2015, 137, 12199-12202.	6.6	52
161	Surface-charge-induced orientation of interfacial water suppresses heterogeneous ice nucleation on <i>α</i> -alumina (0001). Atmospheric Chemistry and Physics, 2017, 17, 7827-7837.	1.9	52
162	Synthesis of Nonplanar Graphene Nanoribbon with Fjord Edges. Journal of the American Chemical Society, 2021, 143, 5654-5658.	6.6	52

#	Article	IF	CITATIONS
163	Electrical tunability of terahertz nonlinearity in graphene. Science Advances, 2021, 7, .	4.7	52
164	Redoxâ€Active Metaphosphateâ€Like Terminals Enable Highâ€Capacity MXene Anodes for Ultrafast Naâ€lon Storage. Advanced Materials, 2022, 34, e2108682.	11.1	52
165	Real time chemical dynamics at surfaces. Surface Science, 2002, 500, 475-499.	0.8	51
166	Ultrafast energy flow in model biological membranes. New Journal of Physics, 2007, 9, 390-390.	1.2	51
167	Bottom-Up, On-Surface-Synthesized Armchair Graphene Nanoribbons for Ultra-High-Power Micro-Supercapacitors. Journal of the American Chemical Society, 2020, 142, 17881-17886.	6.6	51
168	A Curved Graphene Nanoribbon with Multi-Edge Structure and High Intrinsic Charge Carrier Mobility. Journal of the American Chemical Society, 2020, 142, 18293-18298.	6.6	50
169	Vibrational couplings and energy transfer pathways of water's bending mode. Nature Communications, 2020, 11, 5977.	5.8	50
170	Near shot-noise limited hyperspectral stimulated Raman scattering spectroscopy using low energy lasers and a fast CMOS array. Optics Express, 2013, 21, 15113.	1.7	49
171	Orientational Distribution of Free O-H Groups of Interfacial Water is Exponential. Physical Review Letters, 2018, 121, 246101.	2.9	49
172	Hydration strongly affects the molecular and electronic structure of membrane phospholipids. Journal of Chemical Physics, 2012, 136, 114709.	1.2	48
173	Density-dependent electron scattering in photoexcited GaAs in strongly diffusive regime. Applied Physics Letters, 2013, 102, 231120.	1.5	48
174	Enhanced Kinetics of Hole Transfer and Electrocatalysis during Photocatalytic Oxygen Evolution by Cocatalyst Tuning. ACS Catalysis, 2016, 6, 4117-4126.	5.5	48
175	Hot-band excitation of CO chemisorbed on Ru(001) studied with broadband-IR sum-frequency generation. Chemical Physics Letters, 2000, 325, 139-145.	1.2	47
176	In Situ Quantitative Measurement of Concentration Profiles in a Microreactor with Submicron Resolution Using Multiplex CARS Microscopy. Journal of the American Chemical Society, 2008, 130, 11592-11593.	6.6	47
177	Spectroscopic Studies of Electron Injection in Quantum Dot Sensitized Mesoporous Oxide Films. Journal of Physical Chemistry C, 2010, 114, 18866-18873.	1.5	47
178	Communication: Interfacial water structure revealed by ultrafast two-dimensional surface vibrational spectroscopy. Journal of Chemical Physics, 2011, 135, 021101.	1.2	47
179	Hydration Dynamics of Hyaluronan and Dextran. Biophysical Journal, 2012, 103, L10-L12.	0.2	47
180	Structure from Dynamics: Vibrational Dynamics of Interfacial Water as a Probe of Aqueous Heterogeneity. Journal of Physical Chemistry B, 2018, 122, 3667-3679.	1.2	47

#	Article	IF	CITATIONS
181	On the mechanism of charge transport in pentacene. Journal of Chemical Physics, 2008, 129, 044704.	1.2	46
182	Calcium-Induced Molecular Rearrangement of Peptide Folds Enables Biomineralization of Vaterite Calcium Carbonate. Journal of the American Chemical Society, 2018, 140, 2793-2796.	6.6	46
183	Definition of Free O–H Groups of Water at the Air–Water Interface. Journal of Chemical Theory and Computation, 2018, 14, 357-364.	2.3	46
184	Hydration of Sodium Alginate in Aqueous Solution. Macromolecules, 2014, 47, 771-776.	2.2	45
185	Excess Hydrogen Bond at the Ice-Vapor Interface around 200ÂK. Physical Review Letters, 2017, 119, 133003.	2.9	45
186	Photoconductivity Multiplication in Semiconducting Few-Layer MoTe ₂ . Nano Letters, 2020, 20, 5807-5813.	4.5	45
187	Adsorption and dissociation of NO on stepped Pt (533). Journal of Chemical Physics, 2004, 121, 7946.	1.2	44
188	Free carrier photogeneration in polythiophene versus poly(phenylene vinylene) studied with THz spectroscopy. Chemical Physics Letters, 2006, 432, 441-445.	1.2	44
189	<i>Ab Initio</i> Liquid Water Dynamics in Aqueous TMAO Solution. Journal of Physical Chemistry B, 2015, 119, 10597-10606.	1.2	44
190	Nanoscale Distribution of Sulfonic Acid Groups Determines Structure and Binding of Water in Nafion Membranes. Angewandte Chemie - International Edition, 2016, 55, 4011-4015.	7.2	44
191	Surface Potential of a Planar Charged Lipid–Water Interface. What Do Vibrating Plate Methods, Second Harmonic and Sum Frequency Measure?. Journal of Physical Chemistry Letters, 2018, 9, 5685-5691.	2.1	44
192	Direct measurement of phase coexistence in DPPC/cholesterol vesicles using Raman spectroscopy. Chemistry and Physics of Lipids, 2007, 146, 76-84.	1.5	43
193	Serotonin transporter knockout and repeated social defeat stress: Impact on neuronal morphology and plasticity in limbic brain areas. Behavioural Brain Research, 2011, 220, 42-54.	1.2	43
194	Trap-Free Hot Carrier Relaxation in Lead–Halide Perovskite Films. Journal of Physical Chemistry C, 2017, 121, 11201-11206.	1.5	43
195	Accessing the Accuracy of Density Functional Theory through Structure and Dynamics of the Water–Air Interface. Journal of Physical Chemistry Letters, 2019, 10, 4914-4919.	2.1	43
196	Hot-Carrier Cooling in High-Quality Graphene Is Intrinsically Limited by Optical Phonons. ACS Nano, 2021, 15, 11285-11295.	7.3	43
197	Outstanding Charge Mobility by Band Transport in Two-Dimensional Semiconducting Covalent Organic Frameworks. Journal of the American Chemical Society, 2022, 144, 7489-7496.	6.6	43
198	Femtosecond dynamics of chemical reactions at surfaces. Applied Physics A: Materials Science and Processing, 2000, 71, 477-483.	1.1	42

#	Article	IF	CITATIONS
199	Deposition and crystallization studies of thin amorphous solid water films on Ru(0001) and on CO-precovered Ru(0001). Journal of Chemical Physics, 2007, 127, 094703.	1.2	42
200	π ⁺ –π ⁺ stacking of imidazolium cations enhances molecular layering of room temperature ionic liquids at their interfaces. Physical Chemistry Chemical Physics, 2017, 19, 2850-2856.	1.3	42
201	Detection of deep-subwavelength dielectric layers at terahertz frequencies using semiconductor plasmonic resonators. Optics Express, 2012, 20, 5052.	1.7	41
202	Ionic Liquids: Not only Structurally but also Dynamically Heterogeneous. Angewandte Chemie - International Edition, 2015, 54, 687-690.	7.2	41
203	Nature of Excess Hydrated Proton at the Water–Air Interface. Journal of the American Chemical Society, 2020, 142, 945-952.	6.6	41
204	Charge transport mechanism in networks of armchair graphene nanoribbons. Scientific Reports, 2020, 10, 1988.	1.6	41
205	Exceptional electron conduction in two-dimensional covalent organic frameworks. CheM, 2021, 7, 3309-3324.	5.8	41
206	Molecular Restructuring of Water and Lipids upon the Interaction of DNA with Lipid Monolayers. Journal of the American Chemical Society, 2010, 132, 8037-8047.	6.6	40
207	Engineering Proteins at Interfaces: From Complementary Characterization to Material Surfaces with Designed Functions. Angewandte Chemie - International Edition, 2018, 57, 12626-12648.	7.2	40
208	Highly Mobile Large Polarons in Black Phase CsPbl ₃ . ACS Energy Letters, 2021, 6, 568-573.	8.8	40
209	Band transport by large Fröhlich polarons in MXenes. Nature Physics, 2022, 18, 544-550.	6.5	40
210	No Ice-Like Water at Aqueous Biological Interfaces. Biointerphases, 2012, 7, 20.	0.6	39
211	Surface tension of ab initio liquid water at the water-air interface. Journal of Chemical Physics, 2016, 144, 204705.	1.2	39
212	Molecular Modeling of Water Interfaces: From Molecular Spectroscopy to Thermodynamics. Journal of Physical Chemistry B, 2016, 120, 3785-3796.	1.2	39
213	Trimethylamine- <i>N</i> -oxide: its hydration structure, surface activity, and biological function, viewed by vibrational spectroscopy and molecular dynamics simulations. Physical Chemistry Chemical Physics, 2017, 19, 6909-6920.	1.3	39
214	Correlated interfacial water transport and proton conductivity in perfluorosulfonic acid membranes. Proceedings of the National Academy of Sciences of the United States of America, 2019, 116, 8715-8720.	3.3	39
215	Femtosecond time-resolved vibrational SFG spectroscopy of CO/Ru(). Surface Science, 2002, 502-503, 304-312.	0.8	38
216	Dissecting Hofmeister Effects: Direct Anion–Amide Interactions Are Weaker than Cation–Amide Binding. Angewandte Chemie - International Edition, 2016, 55, 8125-8128.	7.2	38

#	Article	IF	CITATIONS
217	Microscale spatial heterogeneity of protein structural transitions in fibrin matrices. Science Advances, 2016, 2, e1501778.	4.7	38
218	Unveiling Heterogeneity of Interfacial Water through the Water Bending Mode. Journal of Physical Chemistry Letters, 2019, 10, 6936-6941.	2.1	38
219	A Nanographeneâ€Based Twoâ€Dimensional Covalent Organic Framework as a Stable and Efficient Photocatalyst. Angewandte Chemie - International Edition, 2022, 61, .	7.2	38
220	A Highly Luminescent Nitrogen-Doped Nanographene as an Acid- and Metal-Sensitive Fluorophore for Optical Imaging. Journal of the American Chemical Society, 2021, 143, 10403-10412.	6.6	37
221	Ultrafast charge generation in a semiconducting polymer studied withTHzemission spectroscopy. Physical Review B, 2004, 70, .	1.1	36
222	Femtosecond time-resolved and two-dimensional vibrational sum frequency spectroscopic instrumentation to study structural dynamics at interfaces. Review of Scientific Instruments, 2008, 79, 093907.	0.6	36
223	Single substitutional nitrogen defects revealed as electron acceptor states in diamond using ultrafast spectroscopy. Physical Review B, 2011, 84, .	1.1	36
224	Repelling and ordering: the influence of poly(ethylene glycol) on protein adsorption. Physical Chemistry Chemical Physics, 2017, 19, 28182-28188.	1.3	36
225	Tunable Superstructures of Dendronized Graphene Nanoribbons in Liquid Phase. Journal of the American Chemical Society, 2019, 141, 10972-10977.	6.6	36
226	Lateral interactions between adsorbed molecules: Investigations of CO on Ru(001) using nonlinear surface vibrational spectroscopies. Physical Review B, 2002, 65, .	1.1	35
227	Imaging of chemical and physical state of individual cellular lipid droplets using multiplex CARS microscopy. Journal of Raman Spectroscopy, 2009, 40, 763-769.	1.2	35
228	Chemical imaging of lipid droplets in muscle tissues using hyperspectral coherent Raman microscopy. Histochemistry and Cell Biology, 2014, 141, 263-273.	0.8	35
229	Nanographenes: Ultrastable, Switchable, and Bright Probes for Superâ€Resolution Microscopy. Angewandte Chemie - International Edition, 2020, 59, 496-502.	7.2	35
230	Quantifying Surfactant Alkyl Chain Orientation and Conformational Order from Sum Frequency Generation Spectra of CH Modes at the Surfactant–Water Interface. Journal of Physical Chemistry Letters, 2014, 5, 3737-3741.	2.1	34
231	Molecular Dynamics Simulations of SFG Librational Modes Spectra of Water at the Water–Air Interface. Journal of Physical Chemistry C, 2016, 120, 18665-18673.	1.5	34
232	The Structure of the Diatom Silaffin Peptide R5 within Freestanding Twoâ€Dimensional Biosilica Sheets. Angewandte Chemie - International Edition, 2017, 56, 8277-8280.	7.2	34
233	Vibrational Coupling between Organic and Inorganic Sublattices of Hybrid Perovskites. Angewandte Chemie - International Edition, 2018, 57, 13657-13661.	7.2	34
234	Evidence for auto-catalytic mineral dissolution from surface-specific vibrational spectroscopy. Nature Communications, 2018, 9, 3316.	5.8	34

#	Article	IF	CITATIONS
235	Polarization-Resolved Broad-Bandwidth Sum-Frequency Generation Spectroscopy of Monolayer Relaxationâ€. Journal of Physical Chemistry C, 2007, 111, 8878-8883.	1.5	33
236	Duramycin-Induced Destabilization of a Phosphatidylethanolamine Monolayer at the Airâ^'Water Interface Observed by Vibrational Sum-Frequency Generation Spectroscopy. Langmuir, 2010, 26, 16055-16062.	1.6	33
237	Polylactideâ€ <i>block</i> â€Polypeptideâ€ <i>block</i> â€Polylactide Copolymer Nanoparticles with Tunable Cleavage and Controlled Drug Release. Advanced Functional Materials, 2014, 24, 4026-4033.	7.8	33
238	Biomimetic Growth of Ultrathin Silica Sheets Using Artificial Amphiphilic Peptides. Advanced Materials Interfaces, 2015, 2, 1500282.	1.9	33
239	Unveiling the Amphiphilic Nature of TMAO by Vibrational Sum Frequency Generation Spectroscopy. Journal of Physical Chemistry C, 2016, 120, 17435-17443.	1.5	33
240	Water-Dispersed High-Quality Graphene: A Green Solution for Efficient Energy Storage Applications. ACS Nano, 2019, 13, 9431-9441.	7.3	33
241	Hydration and Orientation of Carbonyl Groups in Oppositely Charged Lipid Monolayers on Water. Journal of Physical Chemistry B, 2019, 123, 1085-1089.	1.2	33
242	Electrostatic Interactions Control the Functionality of Bacterial Ice Nucleators. Journal of the American Chemical Society, 2020, 142, 6842-6846.	6.6	33
243	Sovagoet al.Reply:. Physical Review Letters, 2008, 101, .	2.9	32
244	Reversible Optical Control of Monolayers on Water through Photoswitchable Lipids. Journal of Physical Chemistry B, 2011, 115, 2294-2302.	1.2	32
245	Uptake of Gold Nanoparticles in Healthy and Tumor Cells Visualized by Nonlinear Optical Microscopy. Journal of Physical Chemistry B, 2011, 115, 5008-5016.	1.2	32
246	Enhancement of the vibrational relaxation rate of surface hydroxyls through hydrogen bonds with adsorbates. Chemical Physics Letters, 1995, 233, 309-314.	1.2	31
247	Interface–solvent effects during colloidal phase transitions. Journal of Physics Condensed Matter, 2005, 17, S3469-S3479.	0.7	31
248	Efficient formation of excitons in a dense electron-hole plasma at room temperature. Physical Review B, 2015, 92, .	1.1	31
249	Perspective on terahertz spectroscopy of graphene. Europhysics Letters, 2015, 111, 67001.	0.7	31
250	Ultrafast Vibrational Dynamics of Water Disentangled by Reverse Nonequilibrium <i>AbÂlnitio</i> Molecular Dynamics Simulations. Physical Review X, 2015, 5, .	2.8	31
251	Macroscopic conductivity of aqueous electrolyte solutions scales with ultrafast microscopic ion motions. Nature Communications, 2020, 11, 1611.	5.8	31
252	Vibrational Dephasing Mechanisms in Hydrogen-Bonded Systems. Physical Review Letters, 1996, 76, 2440-2443.	2.9	30

#	Article	IF	CITATIONS
253	Frequency- and time-domain femtosecond vibrational sum frequency generation from CO adsorbed on Pt(111). Journal of Chemical Physics, 2004, 121, 10174-10180.	1.2	30
254	Measuring Molecular Reorientation at Liquid Surfaces with Time-Resolved Sum-Frequency Spectroscopy: A Theoretical Framework. Journal of Physical Chemistry B, 2009, 113, 7564-7573.	1.2	30
255	Influence of surface polarity on water dynamics at the water/rutile TiO ₂ (110) interface. Journal of Physics Condensed Matter, 2014, 26, 244102.	0.7	30
256	Multimodal Spectroscopic Study of Amyloid Fibril Polymorphism. Journal of Physical Chemistry B, 2016, 120, 8809-8817.	1.2	30
257	Morphological change during crystallization of thin amorphous solid water films on Ru(0001). Journal of Chemical Physics, 2007, 126, 181103.	1.2	29
258	Formation of Lysozyme Oligomers at Model Cell Membranes Monitored with Sum Frequency Generation Spectroscopy. Langmuir, 2014, 30, 7736-7744.	1.6	29
259	SAP(E) – A cell-penetrating polyproline helix at lipid interfaces. Biochimica Et Biophysica Acta - Biomembranes, 2016, 1858, 2028-2034.	1.4	29
260	Oppositely Charged Ions at Water–Air and Water–Oil Interfaces: Contrasting the Molecular Picture with Thermodynamics. Journal of Physical Chemistry Letters, 2016, 7, 825-830.	2.1	29
261	Surface-Specific Spectroscopy of Water at a Potentiostatically Controlled Supported Graphene Monolayer. Journal of Physical Chemistry C, 2019, 123, 24031-24038.	1.5	29
262	Fast energy delocalization upon vibrational relaxation of a deuterated zeolite surface hydroxyl. Journal of Chemical Physics, 1995, 102, 2181-2186.	1.2	28
263	Dynamical Studies of Zeolitic Protons and Adsorbates by Picosecond Infrared Spectroscopy. Catalysis Reviews - Science and Engineering, 1998, 40, 127-173.	5.7	28
264	Spectroscopic analysis of the oxygenation state of hemoglobin using coherent anti-Stokes Raman scattering. Journal of Biomedical Optics, 2006, 11, 050502.	1.4	28
265	Hydrogen Bond Dynamics in Primary Alcohols: A Femtosecond Infrared Study. Journal of Physical Chemistry B, 2015, 119, 1558-1566.	1.2	28
266	Reversible Photochemical Control of Doping Levels in Supported Graphene. Journal of Physical Chemistry C, 2017, 121, 4083-4091.	1.5	28
267	Ultraâ€Narrow Lowâ€Bandgap Graphene Nanoribbons from Bromoperylenes—Synthesis and Terahertz‧pectroscopy. Chemistry - A European Journal, 2017, 23, 4870-4875.	1.7	28
268	The Surface Activity of the Hydrated Proton Is Substantially Higher than That of the Hydroxide Ion. Angewandte Chemie - International Edition, 2019, 58, 15636-15639.	7.2	28
269	Role of Water in CaCO ₃ Biomineralization. Journal of the American Chemical Society, 2021, 143, 1758-1762.	6.6	28
270	Between a hydrogen and a covalent bond. Science, 2021, 371, 123-124.	6.0	28

#	Article	IF	CITATIONS
271	Cove-Edged Graphene Nanoribbons with Incorporation of Periodic Zigzag-Edge Segments. Journal of the American Chemical Society, 2022, 144, 228-235.	6.6	28
272	Ultrafast vibrational dynamics of interfacial water. Chemical Physics, 2008, 350, 23-30.	0.9	27
273	Suppression of Proton Mobility by Hydrophobic Hydration. Journal of the American Chemical Society, 2009, 131, 17070-17071.	6.6	27
274	(Multi)exciton Dynamics and Exciton Polarizability in Colloidal InAs Quantum Dots. Journal of Physical Chemistry C, 2010, 114, 6318-6324.	1.5	27
275	Host–Guest Geometry in Pores of Zeolite ZSMâ€5 Spatially Resolved with Multiplex CARS Spectromicroscopy. Angewandte Chemie - International Edition, 2012, 51, 1343-1347.	7.2	27
276	Perilipin 5 mediated lipid droplet remodelling revealed by coherent Raman imaging. Integrative Biology (United Kingdom), 2015, 7, 467-476.	0.6	27
277	Controlled Folding of Graphene: GraFold Printing. Nano Letters, 2015, 15, 857-863.	4.5	27
278	Determination of Absolute Orientation of Protein α-Helices at Interfaces Using Phase-Resolved Sum Frequency Generation Spectroscopy. Journal of Physical Chemistry Letters, 2017, 8, 3101-3105.	2.1	27
279	Large Hydrogen-Bond Mismatch between TMAO and Urea Promotes Their Hydrophobic Association. CheM, 2018, 4, 2615-2627.	5.8	27
280	Interplay Between Structure, Stoichiometry, and Electron Transfer Dynamics in SILAR-based Quantum Dot-Sensitized Oxides. Nano Letters, 2014, 14, 5780-5786.	4.5	26
281	Ultrafast Reorientational Dynamics of Leucine at the Air–Water Interface. Journal of the American Chemical Society, 2016, 138, 5226-5229.	6.6	26
282	Water in Contact with a Cationic Lipid Exhibits Bulklike Vibrational Dynamics. Journal of Physical Chemistry B, 2016, 120, 10069-10078.	1.2	26
283	Use of Ion Exchange To Regulate the Heterogeneous Ice Nucleation Efficiency of Mica. Journal of the American Chemical Society, 2020, 142, 17956-17965.	6.6	26
284	Femtosecond sum frequency generation at the metal–liquid interface. Surface Science, 2005, 593, 79-88.	0.8	25
285	Sticky water surfaces: Helix–coil transitions suppressed in a cell-penetrating peptide at the air-water interface. Journal of Chemical Physics, 2014, 141, 22D517.	1.2	24
286	Nanoparticle amount, and not size, determines chain alignment and nonlinear hardening in polymer nanocomposites. Proceedings of the National Academy of Sciences of the United States of America, 2017, 114, E3170-E3177.	3.3	24
287	Toward Understanding Bacterial Ice Nucleation. Journal of Physical Chemistry B, 2022, 126, 1861-1867.	1.2	24
288	High-frequency dielectric relaxation of liquid crystals: THz time-domain spectroscopy of liquid crystal colloids. Optics Express, 2006, 14, 11433.	1.7	23

#	Article	IF	CITATIONS
289	Vibrational and orientational dynamics of water in aqueous hydroxide solutions. Journal of Chemical Physics, 2011, 135, 124517.	1.2	23
290	Real-time study of on-water chemistry: Surfactant monolayer-assisted growth of a crystalline quasi-2D polymer. CheM, 2021, 7, 2758-2770.	5.8	23
291	Dynamics of Infrared Photodissociation of Methanol Clusters in Zeolites and in Solution. The Journal of Physical Chemistry, 1996, 100, 15301-15304.	2.9	22
292	A quantitative comparison between reflection absorption infrared and sum-frequency generation spectroscopy. Chemical Physics Letters, 2005, 412, 152-157.	1.2	22
293	Ultrafast inter- and intramolecular vibrational energy transfer between molecules at interfaces studied by time- and polarization-resolved SFG spectroscopy. Physical Chemistry Chemical Physics, 2010, 12, 12909.	1.3	22
294	Tracing Catalytic Conversion on Single Zeolite Crystals in 3D with Nonlinear Spectromicroscopy. Journal of the American Chemical Society, 2012, 134, 1124-1129.	6.6	22
295	Coordination Polymer Framework Based Onâ€Chip Microâ€Supercapacitors with AC Lineâ€Filtering Performance. Angewandte Chemie, 2017, 129, 3978-3982.	1.6	22
296	Accurate terahertz spectroscopy of supported thin films by precise substrate thickness correction. Optics Letters, 2018, 43, 447.	1.7	22
297	Bandâ€Like Charge Transport in Phytic Acidâ€Đoped Polyaniline Thin Films. Advanced Functional Materials, 2021, 31, 2105184.	7.8	22
298	Role of Ion-Pairs in BrÃ,nsted Acid Catalysis. ACS Catalysis, 2015, 5, 6630-6633.	5.5	21
299	Biomimetic vaterite formation at surfaces structurally templated by oligo(glutamic acid) peptides. Chemical Communications, 2015, 51, 15902-15905.	2.2	21
300	Reduced Near-Resonant Vibrational Coupling at the Surfaces of Liquid Water and Ice. Journal of Physical Chemistry Letters, 2018, 9, 1290-1294.	2.1	21
301	Efficient Hot Electron Transfer in Quantum Dot-Sensitized Mesoporous Oxides at Room Temperature. Nano Letters, 2018, 18, 5111-5115.	4.5	21
302	Highly mobile hot holes in Cs ₂ AgBiBr ₆ double perovskite. Science Advances, 2021, 7, eabj9066.	4.7	21
303	Ultrafast Surface Dynamics Studied with Femtosecond Sum Frequency Generation. Journal of Physical Chemistry A, 2001, 105, 1683-1686.	1.1	20
304	Mobility of haloforms on ice surfaces. Chemical Physics Letters, 2004, 385, 244-248.	1.2	20
305	Theory of sum-frequency generation spectroscopy of adsorbed molecules using the density matrix method—broadband vibrational sum-frequency generation and applications. Journal of Physics Condensed Matter, 2005, 17, S201-S220.	0.7	20
306	Multiscale Effects of Interfacial Polymer Confinement in Silica Nanocomposites. Macromolecules, 2015, 48, 7929-7937.	2.2	20

#	Article	IF	CITATIONS
307	Hydrogen bonding and vibrational energy relaxation of interfacial water: A full DFT molecular dynamics simulation. Journal of Chemical Physics, 2017, 147, 044707.	1.2	20
308	Specific Ion–Protein Interactions Influence Bacterial Ice Nucleation. Chemistry - A European Journal, 2021, 27, 7402-7407.	1.7	20
309	Theory of bulk, surface and interface phase transition kinetics in thin films. Journal of Chemical Physics, 2004, 121, 1038-1049.	1.2	19
310	Conical Ionic Amphiphiles Endowed with Micellization Ability but Lacking Air–Water and Oil–Water Interfacial Activity. Journal of the American Chemical Society, 2017, 139, 7677-7680.	6.6	19
311	Time-Resolved Sum Frequency Generation Spectroscopy: A Quantitative Comparison Between Intensity and Phase-Resolved Spectroscopy. Journal of Physical Chemistry A, 2018, 122, 2401-2410.	1.1	19
312	Counteracting Interfacial Energetics for Wetting of Hydrophobic Surfaces in the Presence of Surfactants. Langmuir, 2018, 34, 12344-12349.	1.6	19
313	How surface-specific is 2nd-order non-linear spectroscopy?. Journal of Chemical Physics, 2019, 151, 230901.	1.2	19
314	Liquid flow reversibly creates a macroscopic surface charge gradient. Nature Communications, 2021, 12, 4102.	5.8	19
315	Solution-Processed Graphene–Nanographene van der Waals Heterostructures for Photodetectors with Efficient and Ultralong Charge Separation. Journal of the American Chemical Society, 2021, 143, 17109-17116.	6.6	19
316	Structure and dynamics of interfacial water in model lung surfactants. Faraday Discussions, 2009, 141, 145-159.	1.6	18
317	Biocompatible Polylactide-block-Polypeptide-block-Polylactide Nanocarrier. Biomacromolecules, 2013, 14, 1572-1577.	2.6	18
318	Observation of Water Separated Ion-Pairs between Cations and Phospholipid Headgroups. Journal of Physical Chemistry B, 2014, 118, 4397-4403.	1.2	18
319	Peptide-Controlled Assembly of Macroscopic Calcium Oxalate Nanosheets. Journal of Physical Chemistry Letters, 2019, 10, 2170-2174.	2.1	18
320	Highly Crystalline and Semiconducting Imineâ€Based Twoâ€Dimensional Polymers Enabled by Interfacial Synthesis. Angewandte Chemie, 2020, 132, 6084-6092.	1.6	18
321	Disentangling Sum-Frequency Generation Spectra of the Water Bending Mode at Charged Aqueous Interfaces. Journal of Physical Chemistry B, 2021, 125, 7060-7067.	1.2	18
322	Wettability of graphene, water contact angle, and interfacial water structure. CheM, 2022, 8, 1187-1200.	5.8	18
323	Solvent-dependent vibrational relaxation pathways after successive resonant IR excitation to Ï = 2. Chemical Physics Letters, 1996, 249, 81-86.	1.2	17
324	Nitrated Fatty Acids Modulate the Physical Properties of Model Membranes and the Structure of Transmembrane Proteins. Chemistry - A European Journal, 2017, 23, 9690-9697.	1.7	17

#	Article	IF	CITATIONS
325	Unraveling the Origin of the Apparent Charge of Zwitterionic Lipid Layers. Journal of Physical Chemistry Letters, 2019, 10, 6355-6359.	2.1	17
326	Interfacial Conformation of Hydrophilic Polyphosphoesters Affects Blood Protein Adsorption. ACS Applied Materials & amp; Interfaces, 2019, 11, 1624-1629.	4.0	17
327	Inhibition of Bacterial Ice Nucleators Is Not an Intrinsic Property of Antifreeze Proteins. Journal of Physical Chemistry B, 2020, 124, 4889-4895.	1.2	17
328	Ice Recrystallization Inhibition Is Insufficient to Explain Cryopreservation Abilities of Antifreeze Proteins. Biomacromolecules, 2022, 23, 1214-1220.	2.6	17
329	High-Performance Humidity Sensing in π-Conjugated Molecular Assemblies through the Engineering of Electron/Proton Transport and Device Interfaces. Journal of the American Chemical Society, 2022, 144, 2546-2555.	6.6	17
330	Highly Efficient Ultrafast Energy Transfer into Molecules at Surface Step Sites. Journal of Physical Chemistry C, 2007, 111, 6149-6153.	1.5	16
331	Assessing Charge Carrier Trapping in Silicon Nanowires Using Picosecond Conductivity Measurements. Nano Letters, 2012, 12, 3821-3827.	4.5	16
332	Loosening Quantum Confinement: Observation of Real Conductivity Caused by Hole Polarons in Semiconductor Nanocrystals Smaller than the Bohr Radius. Nano Letters, 2012, 12, 4937-4942.	4.5	16
333	Terahertz Depolarization Effects in Colloidal TiO ₂ Films Reveal Particle Morphology. Journal of Physical Chemistry C, 2014, 118, 1191-1197.	1.5	16
334	Interaction of a Patterned Amphiphilic Polyphenylene Dendrimer with a Lipid Monolayer: Electrostatic Interactions Dominate. Langmuir, 2015, 31, 1980-1987.	1.6	16
335	Kinetic Ionic Permeation and Interfacial Doping of Supported Graphene. Nano Letters, 2019, 19, 9029-9036.	4.5	16
336	Probing fibrin's molecular response to shear and tensile deformation with coherent Raman microscopy. Acta Biomaterialia, 2021, 121, 383-392.	4.1	16
337	Water Orientation at the Calcite-Water Interface. Journal of Physical Chemistry Letters, 2021, 12, 7605-7611.	2.1	16
338	Molecularly Engineered Black Phosphorus Heterostructures with Improved Ambient Stability and Enhanced Charge Carrier Mobility. Advanced Materials, 2021, 33, e2105694.	11.1	16
339	Dephasing of vibrationally excited molecules at surfaces: CO/Ru(001). Chemical Physics Letters, 2004, 388, 269-273.	1.2	15
340	Simultaneous ultrafast probing of intramolecular vibrations and photoinduced charge carriers in rubrene using broadband time-domain THz spectroscopy. Physical Review B, 2007, 75, .	1.1	15
341	Interfacial Water Facilitates Energy Transfer by Inducing Extended Vibrations in Membrane Lipids. Journal of Physical Chemistry B, 2012, 116, 6455-6460.	1.2	15
342	Structural Properties of gp41 Fusion Peptide at a Model Membrane Interface. Journal of Physical Chemistry B, 2013, 117, 15527-15535.	1.2	15

#	Article	IF	CITATIONS
343	Dynamical heterogeneities of rotational motion in room temperature ionic liquids evidenced by molecular dynamics simulations. Journal of Chemical Physics, 2018, 148, 193811.	1.2	15
344	Phase-Sensitive Sum-Frequency Generation Measurements Using a Femtosecond Nonlinear Interferometer. Journal of Physical Chemistry C, 2019, 123, 7266-7270.	1.5	15
345	Interfacial Water Ordering Is Insufficient to Explain Ice-Nucleating Protein Activity. Journal of Physical Chemistry Letters, 2021, 12, 218-223.	2.1	15
346	On the Wavelength-Dependent Performance of Cr-Doped Silica in Selective Photo-Oxidation. Journal of Physical Chemistry C, 2008, 112, 5471-5475.	1.5	14
347	Coherent anti-Stokes Raman scattering microscopy for quantitative characterization of mixing and flow in microfluidics. Optics Letters, 2009, 34, 211.	1.7	14
348	Carrier multiplication in bulk indium nitride. Applied Physics Letters, 2012, 101, .	1.5	14
349	Probing ultrafast temperature changes of aqueous solutions with coherent terahertz pulses. Optics Letters, 2014, 39, 1717.	1.7	14
350	Quantifying transient interactions between amide groups and the guanidinium cation. Physical Chemistry Chemical Physics, 2015, 17, 28539-28543.	1.3	14
351	Reversible activation of pH-sensitive cell penetrating peptides attached to gold surfaces. Chemical Communications, 2015, 51, 273-275.	2.2	14
352	Label-free <i>in situ</i> imaging of oil body dynamics and chemistry in germination. Journal of the Royal Society Interface, 2016, 13, 20160677.	1.5	14
353	Automated cell segmentation in FIJIÂ $^{ extsf{@}}$ using the DRAQ5 nuclear dye. BMC Bioinformatics, 2019, 20, 39.	1.2	14
354	Dynamics of Dicyanamide in Ionic Liquids is Dominated by Local Interactions. Journal of Physical Chemistry B, 2019, 123, 1831-1839.	1.2	14
355	Surface Charges at the CaF ₂ /Water Interface Allow Very Fast Intermolecular Vibrationalâ€Energy Transfer. Angewandte Chemie - International Edition, 2020, 59, 13116-13121.	7.2	14
356	Electrochemical Deposition of a Singleâ€Crystalline Nanorod Polycyclic Aromatic Hydrocarbon Film with Efficient Charge and Exciton Transport. Angewandte Chemie - International Edition, 2022, 61, .	7.2	14
357	Infrared picosecond transient holeâ€burning studies of the effect of hydrogen bonds on the vibrational line shape. Journal of Chemical Physics, 1996, 105, 3431-3442.	1.2	13
358	Broadband Sum Frequency Generation Spectroscopy to Study Surface Reaction Kinetics:Â A Temperature-Programmed Study of CO Oxidation on Pt(111)â€. Journal of Physical Chemistry B, 2004, 108, 14491-14496.	1.2	13
359	Enhanced Autoionization of Water at Phospholipid Interfaces. Journal of Physical Chemistry C, 2013, 117, 510-514.	1.5	13
360	Bovine and human insulin adsorption at lipid monolayers: a comparison. Frontiers in Physics, 2015, 3, .	1.0	13

#	Article	IF	CITATIONS
361	Background-Free Fourth-Order Sum Frequency Generation Spectroscopy. Journal of Physical Chemistry Letters, 2015, 6, 2114-2120.	2.1	13
362	Correlating Carrier Dynamics and Photocatalytic Hydrogen Generation in Pt Decorated CdSe Tetrapods as a Function of Cocatalyst Size. Journal of Physical Chemistry C, 2017, 121, 13070-13077.	1.5	13
363	LK peptide side chain dynamics at interfaces are independent of secondary structure. Physical Chemistry Chemical Physics, 2017, 19, 28507-28511.	1.3	13
364	The surface affinity of cations depends on both the cations and the nature of the surface. Journal of Chemical Physics, 2019, 150, 044706.	1.2	13
365	How water flips at charged titanium dioxide: an SFC-study on the water–TiO ₂ interface. Physical Chemistry Chemical Physics, 2019, 21, 8956-8964.	1.3	13
366	Untying the Bundles of Solution‣ynthesized Graphene Nanoribbons for Highly Capacitive Micro‣upercapacitors. Advanced Functional Materials, 2022, 32, 2109543.	7.8	13
367	Hot electron transfer from PbSe quantum dots molecularly bridged to mesoporous tin and titanium oxide films. Chemical Physics, 2016, 471, 54-58.	0.9	12
368	Single-crystal <i>I</i> _{<i>h</i>} ice surfaces unveil connection between macroscopic and molecular structure. Proceedings of the National Academy of Sciences of the United States of America, 2017, 114, 5349-5354.	3.3	12
369	<i>In Situ</i> Label-Free Study of Protein Adsorption on Nanoparticles. Journal of Physical Chemistry B, 2021, 125, 9019-9026.	1.2	12
370	Accurate molecular orientation at interfaces determined by multimode polarization-dependent heterodyne-detected sum-frequency generation spectroscopy via multidimensional orientational distribution function. Journal of Chemical Physics, 2022, 156, 094703.	1.2	12
371	Solution Synthesis and Characterization of a Long and Curved Graphene Nanoribbon with Hybrid Cove–Armchair–Gulf Edge Structures. Advanced Science, 2022, 9, e2200708.	5.6	12
372	Probing Carrier Dynamics in <i>sp</i> ³ -Functionalized Single-Walled Carbon Nanotubes with Time-Resolved Terahertz Spectroscopy. ACS Nano, 2022, 16, 9401-9409.	7.3	12
373	Coherent picosecond vibron polaritons as probes of vibrational lifetimes. Optics Communications, 1998, 147, 138-142.	1.0	11
374	TeraHertz Dielectric Relaxation of Biological Water Confined in Model Membranes made of Lyotropic Phospholipids. Molecular Crystals and Liquid Crystals, 2009, 500, 108-117.	0.4	11
375	Optical methods for the study of dynamics in biological membrane models. Surface Science, 2009, 603, 1945-1952.	0.8	11
376	Acetylation dictates the morphology of nanophase biosilica precipitated by a 14â€amino acid leucine–lysine peptide. Journal of Peptide Science, 2017, 23, 141-147.	0.8	11
377	Anionic and cationic Hofmeister effects are non-additive for guanidinium salts. Physical Chemistry Chemical Physics, 2017, 19, 9724-9728.	1.3	11
378	Measuring Intracellular Secondary Structure of a Cell-Penetrating Peptide in Situ. Analytical Chemistry, 2017, 89, 11310-11317.	3.2	11

#	Article	IF	CITATIONS
379	Combining Time-of-Flight Secondary Ion Mass Spectrometry Imaging Mass Spectrometry and CARS Microspectroscopy Reveals Lipid Patterns Reminiscent of Gene Expression Patterns in the Wing Imaginal Disc of <i>Drosophila melanogaster</i> . Analytical Chemistry, 2017, 89, 9664-9670.	3.2	11
380	Quantitative Mapping of Triacylglycerol Chain Length and Saturation Using Broadband CARSÂMicroscopy. Biophysical Journal, 2019, 116, 2346-2355.	0.2	11
381	Interfacial Vibrational Dynamics of Ice I _h and Liquid Water. Journal of the American Chemical Society, 2020, 142, 12005-12009.	6.6	11
382	Decoding the molecular water structure at complex interfaces through surface-specific spectroscopy of the water bending mode. Physical Chemistry Chemical Physics, 2020, 22, 10934-10940.	1.3	11
383	Frequency-domain study of nonthermal gigahertz phonons reveals Fano coupling to charge carriers. Science Advances, 2020, 6, .	4.7	11
384	Polarization-Dependent Heterodyne-Detected Sum-Frequency Generation Spectroscopy as a Tool to Explore Surface Molecular Orientation and Ãngström-Scale Depth Profiling. Journal of Physical Chemistry B, 2022, 126, 6113-6124.	1.2	11
385	Ultrafast Electron-Induced Desorption of Water from Nanometer Amorphous Solid Water Films. Journal of Physical Chemistry B, 2007, 111, 6141-6145.	1.2	10
386	lce Nucleation at the Water–Sapphire Interface: Transient Sum-Frequency Response without Evidence for Transient Ice Phase. Journal of Physical Chemistry C, 2018, 122, 24760-24764.	1.5	10
387	Specific Ion Effects on an Oligopeptide: Bidentate Binding Matters for the Guanidinium Cation. Angewandte Chemie - International Edition, 2019, 58, 332-337.	7.2	10
388	Membranes Are Decisive for Maximum Freezing Efficiency of Bacterial Ice Nucleators. Journal of Physical Chemistry Letters, 2021, 12, 10783-10787.	2.1	10
389	The role of structural order in heterogeneous ice nucleation. Chemical Science, 2022, 13, 5014-5026.	3.7	10
390	Time Dependence of Vibrational Relaxation of Deuterated Hydroxyls in Acidic Zeolites Studies in Surface Science and Catalysis, 1994, 84, 493-500.	1.5	9
391	Multiphonon decay of stretch vibrations in zeolites. Chemical Physics, 1995, 201, 215-225.	0.9	9
392	Electronic charge transport in sapphire studied by optical-pump/THz-probe spectroscopy. , 2004, , .		9
393	The distinct vibrational signature of grain-boundary water in nano-crystalline ice films. Chemical Physics Letters, 2007, 448, 121-126.	1.2	9
394	Index mismatch aberration correction over long working distances using spatial light modulation. Applied Optics, 2012, 51, 8034.	0.9	9
395	Multiscale Self-Assembly of Silicon Quantum Dots into an Anisotropic Three-Dimensional Random Network. Nano Letters, 2016, 16, 1942-1948.	4.5	9
396	Dipolar Molecular Capping in Quantum Dot-Sensitized Oxides: Fermi Level Pinning Precludes Tuning Donor–Acceptor Energetics. ACS Nano, 2017, 11, 4760-4767.	7.3	9

#	Article	IF	CITATIONS
397	, Chemisorption of Atomically Precise 42-Carbon Graphene Quantum Dots on Metal Oxide Films Greatly Accelerates Interfacial Electron Transfer. Journal of Physical Chemistry Letters, 2019, 10, 1431-1436.	2.1	9
398	Comparative Adsorption of Acetone on Water and Ice Surfaces. Angewandte Chemie - International Edition, 2019, 58, 3620-3624.	7.2	9
399	Vibrational mode frequency correction of liquid water in density functional theory molecular dynamics simulations with van der Waals correction. Physical Chemistry Chemical Physics, 2020, 22, 12785-12793.	1.3	9
400	Hysteresis in graphene nanoribbon field-effect devices. Physical Chemistry Chemical Physics, 2020, 22, 5667-5672.	1.3	9
401	Picosecond infrared activation of methanol in acid zeolites. Chemical Physics Letters, 1997, 278, 213-219.	1.2	8
402	Surface Photochemistry of Bromoform on Ice:Â Cross Section and Competing Reaction Pathways. Journal of Physical Chemistry B, 2005, 109, 17574-17578.	1.2	8
403	CARS microscopy for the visualization of micrometer-sized iron oxide MRI contrast agents in living cells. Biomedical Optics Express, 2011, 2, 2470.	1.5	8
404	Self-referenced ultra-broadband transient terahertz spectroscopy using air-photonics. Optics Express, 2016, 24, 10157.	1.7	8
405	Femtosecond-timescale buildup of electron mobility in GaAs observed via ultrabroadband transient terahertz spectroscopy. Applied Physics Letters, 2017, 110, .	1.5	8
406	Electrolytes Change the Interfacial Water Structure but Not the Vibrational Dynamics. Journal of Physical Chemistry B, 2019, 123, 8610-8616.	1.2	8
407	Distinguishing different excitation pathways in two-dimensional terahertz-infrared-visible spectroscopy. Journal of Chemical Physics, 2021, 154, 174201.	1.2	8
408	Interfacial Water Structure of Binary Liquid Mixtures Reflects Nonideal Behavior. Journal of Physical Chemistry B, 2021, 125, 10639-10646.	1.2	8
409	Polarization-Dependent Sum-Frequency Generation Spectroscopy for Ãngstrom-Scale Depth Profiling of Molecules at Interfaces. Physical Review Letters, 2022, 128, .	2.9	8
410	Doubly vibrationally resonant spectroscopy of CO on Ru(001). Surface Science, 2002, 502-503, 123-128.	0.8	7
411	Response to "Comment on â€~Coulomb explosion in femtosecond laser ablation of Si(111)'―[Appl. Phys Lett. 85, 694 (2004)]. Applied Physics Letters, 2004, 85, 696-696.	• 1.5	7
412	Retrieving the susceptibility from time-resolved terahertz experiments. Journal of Chemical Physics, 2007, 127, 094308.	1.2	7
413	Observation of photoactive yellow protein anchored to a modified Au(1 1 1) surface by scanning tunneling microscopy. Chemical Physics Letters, 2009, 472, 113-117.	1.2	7
414	Precision waveguide system for measurement of complex permittivity of liquids at frequencies from 60 to 90ÂGHz. Review of Scientific Instruments, 2011, 82, 104703.	0.6	7

#	Article	IF	CITATIONS
415	Structural Basis for the Polymorphism of \hat{I}^2 -Lactoglobulin Amyloid-Like Fibrils. , 2014, , 333-343.		7
416	Nanoscale Distribution of Sulfonic Acid Groups Determines Structure and Binding of Water in Nafion Membranes. Angewandte Chemie, 2016, 128, 4079-4083.	1.6	7
417	A new force field including charge directionality for TMAO in aqueous solution. Journal of Chemical Physics, 2016, 145, 064103.	1.2	7
418	Tension Causes Unfolding of Intracellular Vimentin Intermediate Filaments. Advanced Biology, 2020, 4, e2000111.	3.0	7
419	Orientation independent vibrational dynamics of lipid-bound interfacial water. Physical Chemistry Chemical Physics, 2020, 22, 10142-10148.	1.3	7
420	Compositionâ€Dependent Passivation Efficiency at the CdS/CuIn 1- x Ga x Se 2 Interface. Advanced Materials, 2020, 32, 1907763.	11.1	7
421	Ice Nucleation Activity of Perfluorinated Organic Acids. Journal of Physical Chemistry Letters, 2021, 12, 3431-3435.	2.1	7
422	Antisurfactant (Autophobic) Behavior of Superspreader Surfactant Solutions. Langmuir, 2021, 37, 6243-6247.	1.6	7
423	Phospholipid acyl tail affects lipid headgroup orientation and membrane hydration. Journal of Chemical Physics, 2022, 156, .	1.2	7
424	Comment on "Ultrafast Laser Excitation ofCO/Pt(111)Probed by Sum Frequency Generation: Coverage Dependent Desorption Efficiency― Physical Review Letters, 2004, 93, 249601; author reply 249602.	2.9	6
425	Adsorption and photochemistry of multilayer bromoform on ice. Surface Science, 2006, 600, 3337-3344.	0.8	6
426	A THz spectrometer based on a CsI prism. Journal of Optics, 2008, 10, 095303.	1.5	6
427	Coherent Anti-Stokes Raman Scattering Microspectroscopic Kinetic Study of Fast Hydrogen Bond Formation in Microfluidic Devices. Analytical Chemistry, 2013, 85, 8923-8927.	3.2	6
428	Full membrane spanning self-assembled monolayers as model systems for UHV-based studies of cell-penetrating peptides. Biointerphases, 2015, 10, 019009.	0.6	6
429	Size-dependent electron transfer from atomically defined nanographenes to metal oxide nanoparticles. Nanoscale, 2020, 12, 16046-16052.	2.8	6
430	Geopolymer-Encapsulated Cesium Lead Bromide Perovskite Nanocrystals for Potential Display Applications. ACS Applied Nano Materials, 2020, 3, 11695-11700.	2.4	6
431	Intrinsically Disordered Osteopontin Fragment Orders During Interfacial Calcium Oxalate Mineralization. Angewandte Chemie - International Edition, 2021, 60, 18577-18581.	7.2	6
432	Low-field onset of Wannier-Stark localization in a polycrystalline hybrid organic inorganic perovskite. Nature Communications, 2021, 12, 5719.	5.8	6

#	Article	IF	CITATIONS
433	Gigahertz Modulation of Femtosecond Time-Resolved Surface Sum-Frequency Generation Due to Acoustic Strain Pulses. Journal of Physical Chemistry C, 2014, 118, 20875-20880.	1.5	5
434	Hofmeisterâ€Effekte unter der Lupe: Die direkte Anionâ€Amidâ€Bindung ist schwäher als die Kationâ€Amidâ€Bindung. Angewandte Chemie, 2016, 128, 8257-8261.	1.6	5
435	Boosting Biexciton Collection Efficiency at Quantum Dot–Oxide Interfaces by Hole Localization at the Quantum Dot Shell. Journal of Physical Chemistry Letters, 2017, 8, 2654-2658.	2.1	5
436	Electron Transfer from Bi-Isonicotinic Acid Emerges upon Photodegradation of N3-Sensitized TiO ₂ Electrodes. ACS Applied Materials & Interfaces, 2017, 9, 35376-35382.	4.0	5
437	Thickness-dependent electron momentum relaxation times in iron films. Applied Physics Letters, 2020, 116, .	1.5	5
438	Tuning interfacial charge transfer in atomically precise nanographene–graphene heterostructures by engineering van der Waals interactions. Journal of Chemical Physics, 2022, 156, 074702.	1.2	5
439	Phase transitions in a lipid monolayer observed with vibrational sum-frequency generation. , 2003, , .		4
440	Both Poly(ethylene glycol) and Poly(methyl ethylene phosphate) Guide Oriented Adsorption of Specific Proteins. Langmuir, 2019, 35, 14092-14097.	1.6	4
441	Nanographene: ultrastabile, schaltbare und helle Sonden für die hochauflösende Mikroskopie. Angewandte Chemie, 2020, 132, 504-510.	1.6	4
442	Interfacial Vibrational Spectroscopy of the Water Bending Mode on Ice <i>I_h</i> . Journal of Physical Chemistry C, 2021, 125, 22937-22942.	1.5	4
443	Membrane Structure of Aquaporin Observed with Combined Experimental and Theoretical Sum Frequency Generation Spectroscopy. Langmuir, 2021, 37, 13452-13459.	1.6	4
444	Dynamical studies of zeolitic protons and interactions with adsorbates by picosecond infrared spectroscopy. Applied Surface Science, 1997, 121-122, 80-88.	3.1	3
445	Ultrafast scattering of electrons in TiO2. , 2004, , 517-520.		3
446	The CO–H interaction on Pt(1 1 1) studied using temperature programmed vibrational sum frequency generation. Chemical Physics Letters, 2005, 412, 482-487.	1.2	3
447	Sum-frequency generation spectroscopy of self-assembled structures of Guanosine 5′-monophosphate on mica. Chemical Physics Letters, 2008, 467, 159-163.	1.2	3
448	Liquid Crystal Colloids Studied by THz Time-Domain Spectroscopy. Molecular Crystals and Liquid Crystals, 2008, 480, 21-28.	0.4	3
449	Thiolated Lysineâ€Leucine Peptides Selfâ€Assemble into Biosilica Nucleation Pits on Gold Surfaces. Advanced Materials Interfaces, 2017, 4, 1700399.	1.9	3
450	Large area conductive nanoaperture arrays with strong optical resonances and spectrally flat terahertz transmission. Applied Physics Letters, 2017, 111, .	1.5	3

#	Article	IF	CITATIONS
451	Engineering von Proteinen an OberflÄ e hen: Von komplementÄ r er Charakterisierung zu MaterialoberflÄ e hen mit maÄŸgeschneiderten Funktionen. Angewandte Chemie, 2018, 130, 12806-12830.	1.6	3
452	Bridging chains mediate nonlinear mechanics of polymer nanocomposites under cyclic deformation. Polymer, 2020, 200, 122529.	1.8	3
453	Untersuchung der Mineralâ€Wasserâ€Grenzschicht mit nichtâ€linearer optischer Spektroskopie. Angewandte Chemie, 2021, 133, 10574-10595.	1.6	3
454	Assembly of iron oxide nanosheets at the air–water interface by leucine–histidine peptides. RSC Advances, 2021, 11, 27965-27968.	1.7	3
455	Protein Nanopore Membranes Prepared by a Simple Langmuir–Schaefer Approach. Small, 2021, 17, e2102975.	5.2	3
456	Electrochemical Deposition of a Single rystalline Nanorod Polycyclic Aromatic Hydrocarbon Film with Efficient Charge and Exciton Transport. Angewandte Chemie, 2022, 134, .	1.6	3
457	Passively Stabilized Phase-Resolved Collinear SFG Spectroscopy Using a Displaced Sagnac Interferometer. Journal of Physical Chemistry A, 2022, 126, 951-956.	1.1	3
458	Solutionâ€Processed Waferâ€Scale Ag ₂ S Thin Films: Synthesis and Excellent Charge Transport Properties. Advanced Functional Materials, 2022, 32, .	7.8	3
459	Acidic pH Promotes Refolding and Macroscopic Assembly of Amyloid β (16–22) Peptides at the Air–Water Interface. Journal of Physical Chemistry Letters, 2022, 13, 6674-6679.	2.1	3
460	Optimizing Vibrational Population Transfer at Surfaces through Infrared Excitation. Bulletin of the Chemical Society of Japan, 2002, 75, 1005-1010.	2.0	2
461	Quantitative multiplex CARS spectroscopy in congested spectral regions. , 2007, , .		2
462	Label-free cellular imaging of lipid composition of individual lipid droplets using multiplex CARS microscopy. Chemistry and Physics of Lipids, 2008, 154, S5.	1.5	2
463	Die Struktur des Silaffinâ€Peptids R5 aus Diatomeen in freistehenden zweidimensionalen BiosilikatwĀ ¤ den. Angewandte Chemie, 2017, 129, 8390-8394.	1.6	2
464	Room-temperature solution-phase epitaxial nucleation of PbS quantum dots on rutile TiO ₂ (100). Nanoscale Advances, 2020, 2, 377-383.	2.2	2
465	Oberflähenladungen an der CaF 2 â€Wasserâ€Grenzflähe erlauben eine sehr schnelle intermolekulare Übertragung von Schwingungsenergie. Angewandte Chemie, 2020, 132, 13217-13222.	1.6	2
466	Two-Dimensional Terahertz-Infrared-Visible Spectroscopy Elucidates Coupling Between Low- and High-Frequency Modes. Springer Series in Optical Sciences, 2019, , 197-214.	0.5	2
467	A Nanographeneâ€Based Twoâ€Dimensional Covalent Organic Framework as a Stable and Efficient Photocatalyst. Angewandte Chemie, 2022, 134, .	1.6	2
468	Generation of incoherent mid-infrared photon echoes with parametrically downconverted light. Optics Letters, 1996, 21, 1579.	1.7	1

MISCHA BONN

#	Article	IF	CITATIONS
469	Infrared holeburning spectroscopy in acid zeolites. Studies in Surface Science and Catalysis, 1997, 105, 567-574.	1.5	1
470	Cascading second-order versus direct third-order nonlinear optical processes in a uniaxial crystal. Optics Communications, 2004, 234, 407-417.	1.0	1
471	Surface Femtochemistry. , 2010, , 203-221.		1
472	Ultrafast dynamics of water at the water-air interface studied by femtosecond surface vibrational spectroscopy. EPJ Web of Conferences, 2013, 41, 06009.	0.1	1
473	Comment on "Enhancement of Second-Order Nonlinear-Optical Signals by Optical Stimulation― Physical Review Letters, 2016, 116, 059401.	2.9	1
474	Dynamics of Water Molecules at the Water/Air Interface. , 2018, , 348-355.		1
475	Das hydratisierte Proton besitzt eine deutlich höhere Oberflähenaktivitäals das Hydroxidion. Angewandte Chemie, 2019, 131, 15783-15786.	1.6	1
476	Sun <i>etÂal.</i> Reply:. Physical Review Letters, 2019, 123, 099602.	2.9	1
477	Charge carrier scattering and ultrafast Auger dynamics in two-dimensional superatomic semiconductors. Applied Physics Letters, 2020, 116, 201109.	1.5	1
478	CHAPTER 11. Carrier Dynamics in Photovoltaic Structures and Materials Studied by Time-Resolved Terahertz Spectroscopy. RSC Energy and Environment Series, 2013, , 301-336.	0.2	1
479	Self-referenced Transient THz Spectroscopy with ABCD Detection. , 2015, , .		1
480	Graphene: The Ultimate Nonlinear Material at Terahertz Frequencies. , 2019, , .		1
481	Ultrafast carrier dynamics in graphene and graphene nanostructures. Terahertz Science & Technology, 2020, 13, 135-148.	0.5	1
482	German Commerical Policy Economica, 1935, 2, 353.	0.9	0
483	Incoherent Mid-Infrared Photon Echoes With Parametrically Downconverted Light. Laser Chemistry, 1999, 19, 123-126.	0.5	0
484	Probing charge carriers in semiconductor quantum dots by terahertz spectroscopy. , 2003, , .		0
485	Geometrical vs. statistical models for describing phase transition kinetics in thin films. Physical Chemistry Chemical Physics, 2004, 6, 5516.	1.3	0
486	THz time-domain spectroscopy of liquid crystal colloids. , 2007, , .		0

0

#	Article	IF	CITATIONS
487	Multiplex coherent anti-Stokes Raman scattering microscopy on lipid droplets in HeLa cells. Proceedings of SPIE, 2007, , .	0.8	0
488	Photoinduced charge-carriers in SrTiO <inf>3</inf> crystals investigated by pump-probe THz spectroscopy. , 2008, , .		0
489	Coherent Anti-Stokes Raman Scattering (CARS) microscopy for three-dimensional flow characterization in microfluidics. , 2008, , .		0
490	Ultrafast intraband relaxation in colloidal quantum dots. , 2008, , .		0
491	Time domain terahertz spectroscopy for investigating the dielectric relaxation dynamics of water in model membranes. , 2010, , .		0
492	Quantitative CARS Spectral Imaging of a Single Living Cell in the Fingerprint Region. , 2010, , .		0
493	Unraveling the Link between Molecular Conformation and Morphology and Mechanics of Amyloid Fibrils. Biophysical Journal, 2013, 104, 553a-554a.	0.2	0
494	Folding and Unfolding of pH Sensitive Peptides: The Role of Interfaces. Biophysical Journal, 2013, 104, 394a.	0.2	0
495	Nonlinear terahertz conductivity in graphene. , 2013, , .		0
496	Photoexcitation cascade and multiple hot carrier generation in graphene. , 2013, , .		0
497	Hot carrier multiplication in graphene. , 2013, , .		0
498	Single-pulse terahertz coherent control of spin resonance in a canted antiferromagnet. , 2013, , .		0
499	Terahertz photoconductivity of graphene nanostructures. , 2013, , .		0
500	Density-dependent electron scattering in photoexcited GaAs. , 2013, , .		0
501	Terahertz Carrier Dynamics in Graphene and Graphene Nanostructures. , 2014, , .		0
502	Inherent Resistivity of Graphene to Strong THz Fields. , 2014, , .		0
503	Nonlinear THz conductivity in graphene. , 2014, , .		0

504 Ultrafast carrier dynamics in graphene and graphene nanostructures. , 2014, , .

#	Article	IF	CITATIONS
505	Amyloid Fibrils: Nanoscale Heterogeneity of the Molecular Structure of Individual hIAPP Amyloid Fibrils Revealed with Tipâ€Enhanced Raman Spectroscopy (Small 33/2015). Small, 2015, 11, 4130-4130.	5.2	Ο
506	Photovoltaic Polymer-Fullerene Blends: Terahertz Carrier Dynamics and Device Performance. , 2015, , .		0
507	Thermodynamic picture of terahertz conduction in graphene. , 2016, , .		0
508	Spin-resolved terahertz spectroscopy. , 2016, , .		0
509	Intense THz-assisted modulation of semiconductor optical properties. , 2018, , .		0
510	Resolution along both infrared and visible frequency axes in second-order Fourier-transform vibrational sum-frequency generation spectroscopy. Chemical Physics, 2018, 512, 27-35.	0.9	0
511	Kopplung von hoch―und niederfrequenten Schwingungsmoden in organischâ€anorganischen Perowskiten. Angewandte Chemie, 2018, 130, 13845-13849.	1.6	Ο
512	Advanced Vibrational Spectroscopies, dedicated to Dr. Edwin J. Heilweil on the occasion of his 60th birthday. Chemical Physics, 2018, 512, 1-2.	0.9	0
513	Control of Terahertz Nonlinearity in Graphene by Gating. , 2019, , .		Ο
514	Vergleichende Acetonadsorption an Wasser―und Eisoberflähen. Angewandte Chemie, 2019, 131, 3659-3663.	1.6	0
515	Spezifische Ionenâ€Effekte am Beispiel eines Oligopeptids: die Rolle zweizäniger Koordination beim Guanidiniumâ€Kation. Angewandte Chemie, 2019, 131, 338-343.	1.6	Ο
516	Rücktitelbild: Nanographene: ultrastabile, schaltbare und helle Sonden für die hochauflösende Mikroskopie (Angew. Chem. 1/2020). Angewandte Chemie, 2020, 132, 516-516.	1.6	0
517	WATER AT INTERFACES: WHERE THEORY NEEDS TO MEET EXPERIMENT. , 2021, , .		Ο
518	Intrinsisch ungeordnete Osteopontinâ€Fragmente ordnen sich wĤrend der interfazialen Calciumoxalatâ€Mineralisierung. Angewandte Chemie, 2021, 133, 18725-18729.	1.6	0
519	THz Pump-Probe Measurements of Electrons in Non-Polar Liquids. Springer Series in Chemical Physics, 2001, , 459-463.	0.2	0
520	Electronic charge transport in single-crystal Al2O3: Transient conductivity and its temperature dependence probed by THz time-domain spectroscopy. , 2002, , .		0
521	Probing transient conductivity in condensed matter by optical pump/THz time-domain spectroscopy. , 2002, , .		0
522	Transient Conductivity in Single-Crystal Al2O3 Probed by THz Time-Domain Spectroscopy. Springer Series in Chemical Physics, 2003, , 262-264.	0.2	0

#	Article	IF	CITATIONS
523	THz spectroscopy of nanostructures. , 2004, , .		0
524	FEMTOSECOND SUM FREQUENCY GENERATION ON MOLECULAR ADSORBATES. , 2004, , .		0
525	Ultrafast 2D-IR spectroscopy of a molecular monolayer. Springer Series in Chemical Physics, 2009, , 511-513.	0.2	0
526	THz Studies of Charge and Exciton Dynamics in Semiconductor Nanostructures. , 2009, , .		0
527	Ultrafast vibrational dynamics of interfacial water. Springer Series in Chemical Physics, 2009, , 517-519.	0.2	0
528	Control of Energy Relaxation Pathways in Graphene: Carrier-Carrier Scattering vs Phonon Emission. , 2015, , .		0
529	Perilipin 5 mediated lipid droplet remodelling revealed by coherent Raman imaging. FASEB Journal, 2015, 29, 568.19.	0.2	0
530	Terahertz Carrier Dynamics in Graphene Nanoribbons with Different Peripherial Functional Groups. , 2016, , .		0
531	Kinetic Ionic Permeation and Interfacial Doping of Supported Graphene Measured with Terahertz Photoconductivity Measurements. , 2020, , .		0